

Novel design methods of central nervous system of *C. elegans* and olfactory bulb model of mammal based on sequential logic and numerical integration

Onodera, Kazuhito

(出版者 / Publisher)

法政大学大学院理工学研究科

(雑誌名 / Journal or Publication Title)

法政大学大学院紀要. 理工学研究科編

(巻 / Volume)

64

(開始ページ / Start Page)

1

(終了ページ / End Page)

6

(発行年 / Year)

2023-03-24

(URL)

<https://doi.org/10.15002/00026336>

Novel design methods of central nervous system of *C. elegans* and olfactory bulb model of mammal based on sequential logic and numerical integration

Kazuhito Onodera

Supervisor: Prof. Hiroyuki Torikai

Graduate School of Science and Engineering, Hosei University

This study proposes a novel design method of a neuromorphic electronic circuit: design of a neuromorphic circuit based on appropriately selected hybrid dynamics of synchronous sequential logic, asynchronous sequential logic, and numerical integration. Based on the proposed design method, a novel central nervous system model of *C. elegans*, and an olfactory bulb model are presented. It is then shown that the presented models can realize typical responses of a conventional central nervous system model of *C. elegans*, and the observation of chaos in the olfactory bulb. Furthermore, the presented models are implemented by a field programmable gate array and the presented model of *C. elegans* is used to control a prototype robot of *C. elegans* body. Then, experiments validate that the presented central nervous system model enables the body robot to reproduce typical chemotaxis behaviors of the conventional *C. elegans* model. In addition, comparisons show that the presented model consumes fewer circuit elements and lower power compared to various central nervous system models of *C. elegans* based on synchronous sequential logic, asynchronous sequential logic, and numerical integration.

Key Words : Hybrid nonlinear dynamics, Asynchronous SL, *C. elegans*, Chemotaxis, FPGA, olfactory bulb,

I. General Introduction

The *C. elegans* in Fig. 1(a) has one of the simplest and the most well understood central nervous systems[2]. In spite of its simple nervous system, the *C. elegans* can perform decision making functions such as chemotaxis behaviors[3]-[7], which cause various movements (e.g., clockwise turning, anticlockwise turning, and random movement) to approach chemoattractant (e.g., food) and to escape from chemorepellent (e.g., poison).

There exist various research projects aiming at designing artificial central nervous system models of the *C. elegans* by electronic circuits[8]-[14], where their motivations include to build fundamental frameworks for developing brain-inspired robotics and brain-inspired computing. For example, Refs. [11][12] design a simplified artificial central nervous system model of the *C. elegans* as shown in Fig. 1(b). Also, Fig. 2 shows a picture of olfactory bulb of mammal [16]. The olfactory bulb model of mammal has been established as a mathematical model based on anatomy and electrophysiology[17]-[23]. In recent years, there have been cases of abnormalities in the sense of smell due to the aftereffects of covid-19 virus. There exist various research projects aiming at designing artificial nose model of mammal by electronic circuits, where their motivations include to build fundamental frameworks for elucidation of the mechanism of brain function including the olfactory bulb. Note that most neuromorphic electronic circuits[15], including the artificial central nervous system circuit of the *C. elegans*

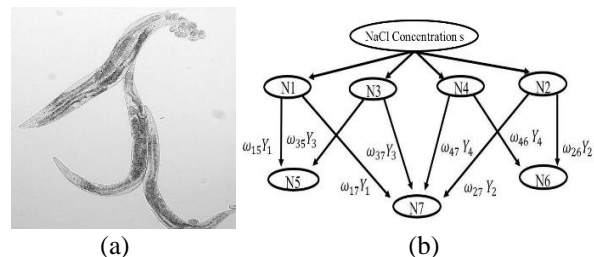


Fig. 1: (a) Picture of *C. elegans*[1]. (b) A simplified central nervous system model of the *C. elegans*[11][12].

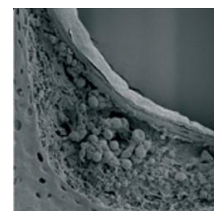


Fig. 2 : Picture of mammal olfactory bulb.

and olfactory bulb model of mammal, have been modeled and implemented based on the following three methods: (1) ordinary differential equation model implemented by analog dynamic circuit, (2) difference equation model implemented by switched capacitor circuit, and (3) numerical integration model implemented by digital signal processor. On the contrary, recently, various neuromorphic electronic circuits based on the novel fourth method have been developed: (4) asynchronous cellular automaton neuromorphic model implemented by asynchronous sequential logic (SL)

[24]-[33]. It has been shown that asynchronous SL neuromorphic circuits have been more hardware-efficient compared to digital signal processor neuromorphic circuits that have been designed based on numerical integrations straightforwardly [24]-[33]. Inspired by the researches on the simplified artificial central nervous system circuits of the *C. elegans* and the hardware-efficient asynchronous SL neuromorphic circuits, in this paper, a novel simplified central nervous system model of the *C. elegans* is presented based on hybrid dynamics of asynchronous SL, synchronous SL, and numerical integration. In addition, this paper aims at comparing the presented model with various central nervous system models based on asynchronous SL, synchronous SL, and numerical integration. The presented model is implemented by a field programmable gate array (FPGA) and it is shown that the presented model can realize typical chemotaxis behaviors of a physically assembled prototype robot of the *C. elegans*. Additionally, it is shown that the presented model is most hardware-efficient in the compared models. Novelty and significance of this paper include the following points:

(a) a neuromorphic circuit based on the hybrid dynamics of asynchronous SL, synchronous SL, and numerical integration is presented in this paper for the first time, and (b) the results of this paper will provide fundamental knowledge about designing hardware-efficient central nervous system models and other brain-inspired processors.

II. A novel simplified *C. elegans* mode

In this section, a novel simplified central nervous system model of the *C. elegans* is presented, where the network structure in Fig. 1(b) [11][12] is used as the structure of the presented model. On the contrary, the dynamics of the model is totally different from that of the model in [11][12], i.e., the presented model is designed based on hybrid dynamics of the following three kinds of dynamical systems, where SL represents sequential logic. This paper treats only a part of the model, and details of the model will be described in my master's thesis.

- Numerical integration (NI) having fixed point number internal states
- Synchronous SL (SSL) having integer internal states and triggered by a single clock
- Asynchronous SL (ASL) having integer internal states and triggered by multiple asynchronous clocks

III. Design of neuron models N_i in *C. elegans* model

Let us define the following sets, where “ \uparrow ” denotes a positive edge of a rectangular-shaped signal. E is the set $\{\uparrow, 0\}$ of the positive edge and zero. F is the set of the signed fixed point numbers with 14-bit integer part and 9-bit decimal part. N_N is the set $\{0, 1, \dots, N\}$ of finite integers. The neuron model N_i , $i \in \{1, 2\}$, has clock input C^{NI} , $C_i^{dif} \in E$ for NI, clock inputs C_i^U , C_i^B , and $C_i^{cel} \in E$ for ASL, stimulation input $s \in F$, and spike

output $Y_i \in E$, where the clocks C^{NI} , C_i^U , C_i^B , C_i^{dif} , and C_i^{cel} have periods T^{NI} , T_i^U , T_i^B , T_i^{dif} , and T_i^{cel} , respectively. The neuron model N_i has the following membrane potential V_i , and internal states.

$$\begin{aligned} V_i, s_i, u_i^d, b_i^d, i_i^d, V_i^{dif} &\in F. \\ U_i^h, B_i^h, P_i^h, Q_i^h, V_i^{cel}, P_i^{cel} &\in N_N. \end{aligned}$$

Let “ $:=$ ” denote an instantaneous state update.

If $V_i < V_i^T$, the neuron model N_i exhibits the following state transitions. NI and ASL hybrid dynamics of neuron model N_i :

If $C^{NI} = \uparrow$, then

$$\begin{cases} s_i := F_i^s(s_i, s), \\ u_i^d := F_i^{ud}(u_i^d, b_i^d, i_i^d), \\ b_i^d := F_i^{bd}(u_i^d, b_i^d, i_i^d), \\ i_i^d := F_i^{id}(u_i^d, b_i^d, i_i^d). \end{cases} \quad (1)$$

If $C_i^U = \uparrow$, then

$$\begin{cases} U_i^h := F_i^{Uh}(U_i^h, P_i^h, B_i^h, s), \\ P_i^h := F_i^{Ph}(U_i^h, P_i^h, B_i^h, s). \end{cases} \quad (2)$$

If $C_i^B = \uparrow$, then

$$\begin{cases} B_i^h := F_i^{Bh}(U_i^h, Q_i^h, B_i^h, s), \\ Q_i^h := F_i^{Qh}(U_i^h, Q_i^h, B_i^h, s). \end{cases} \quad (3)$$

If $C_i^{dif} = \uparrow$, then

$$V_i^{dif} := F_i^{dif}(V_i^{dif}, b_i^d). \quad (4)$$

If $C_i^{cel} = \uparrow$, then

$$\begin{cases} V_i^{cel} := F_i^{cV}(V_i^{cel}, P_i^{cel}, U_i^h), \\ P_i^{cel} := F_i^{cP}(V_i^{cel}, P_i^{cel}, U_i^h). \end{cases} \quad (5)$$

$$V_i = F_i^V(V_i^{dif}, V_i^{cel}). \quad (6)$$

The functions F_i^s, \dots, F_i^V are designed in my master's thesis. The variable s_i is assumed to have a lower bound 10. If $V_i \geq V_i^T$, the neuron model N_i exhibits the following reset.

$$\text{If } C_i^V = \uparrow, \text{ and } V_i \geq V_i^T, \text{ then } V_i := V_0. \quad (7)$$

The neuron model N_i generates the following spike output.

$$Y_i = \begin{cases} 0 & \text{if } V_i < V_i^T \\ \uparrow & \text{if } V_i \geq V_i^T \end{cases} \quad (8)$$

Fig. 3 shows a timing chart of the neuron model N_i . Our extensive analyses revealed that the neuron models N1 and N2 exhibited the following responses (see Fig. 4).

- The neuron model N1 generates spikes $Y_i = \uparrow$ when the input s is increasing in time.
- The neuron model N2 generates spikes $Y_i = \uparrow$ when the input s is decreasing in time.

C. elegans chemotaxis can be realized by a system constructed with such neuron models. Details of the model will be described in my master's thesis.

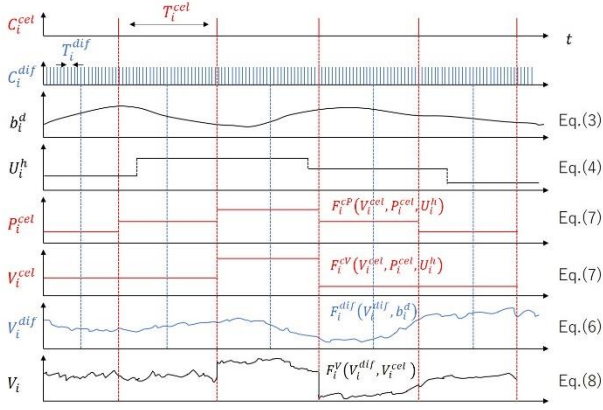


Fig.3 : Timing chart of neuron model N_i , $i \in \{1, 2\}$.

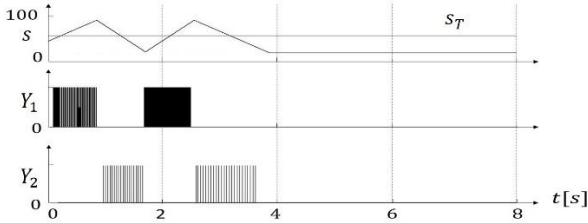


Fig.4 : Simulation result showing responses of the neuron models N_1 and N_2 to the stimulation input s .

IV. Implementation and Comparisons

The dynamic equations of the presented central nervous system model were handwritten as RTL-level Verilog-HDL codes. The set of these Verilog-HDL codes were compiled by Xilinx's design suite Vivado 2020.1 and the resulting bitstream file was downloaded to Xilinx's field programmable gate array (FPGA) device Xc7a200tsbg484-1. It was confirmed that the implemented model exhibited the responses of chemotaxis. For comparison, several central nervous system models of the *C. elegans* were implemented as summarized in Table 1. The model no. 1 is the presented model. The model no. 2 is the most straight forward model, i.e., the differential equations of the central nervous system model in [11] were implemented by numerical integrations (Euler formula) straightforwardly. The other models from no. 3 to no. 10 are modeled by various mixtures of the numerical integration, the synchronous SL, and the asynchronous SL. For fairness of comparison, the bit lengths of the registers of the 10 models were shortened

as short as possible to realize the chemotaxis behaviors. Note that the asynchronous and synchronous SLs are not used in all the models in Table 1. The reason for this is that some nonlinear functions of the neuron models have three or more arguments and thus these functions are not suited to be implemented by look-up tables of SLs. Table 1 shows comparison results. It can be confirmed that the presented model (model no. 1) is the model of choice since it consumes the fewest circuit elements and the lowest power. On the contrary, the straightforward numerical integration model (model no. 2) is the worst choice since it consumes the most circuit elements and the highest power. Note that the nonlinear functions of the neuron model are implemented by look-up tables in the case of the SLs and by multipliers in the case of the numerical integration. Our analyses revealed that nonlinear functions with low resolutions can be used to realize the chemotaxis behaviors of the robot. Therefore, the SLs (with the low resolution functions) are more suitable for implementing the nonlinear vector field of the neuron model compared to the numerical integration (with the multipliers). Note also that our previous research revealed that the asynchronous SL could equivalently realize a higher resolution of a nonlinear vector field compared to the synchronous SL[26]. Therefore, the asynchronous SL is more suited to implement the neuron model compared to the synchronous SL.

V. A novel simplified olfactory bulb model

In this section, a novel simplified olfactory bulb model of mammal is presented, where the system in Ref. [17] is used as the structure of the presented model. On the contrary, the dynamics of the model is totally different from that of the model in [17], i.e., the presented model is designed based on dynamics of the following dynamical systems, where SL represents sequential logic.

- Asynchronous SL (ASL) having integer internal states and triggered by multiple asynchronous clocks

Let us define the following sets, where “ \uparrow ” denotes a positive edge of a rectangular-shaped signal. \mathbf{E} is the set $\{\uparrow, 0\}$ of the positive edge and zero. \mathbf{F} is the set of the signed fixed point numbers. \mathbf{N}_N is the set $\{0, 1, \dots, N\}$ of finite integers. The olfactory bulb model has clock inputs C_m , and $C_g \in \mathbf{E}$ for ASL, stimulation time $t \in \mathbf{F}$, where the clocks C_m , and C_g have periods T_m , and T_g .

Table 1 : Comparisons

Model	Internal sub-dynamics of N1, N2	Membrane dynamics of N1, N2	N3, N4	N5, N6, N7	#LUTs	POW (W)
No. 1	NI, ASL	NI, ASL	SSL	NI, ASL	5396	0.289
No. 2	NI	NI	NI	NI	7368	0.386
No. 3	NI	NI	SSL	NI	6830	0.366
No. 4	NI, ASL	NI, SSL	NI	NI	6383	0.338
No. 5	NI, ASL	NI, ASL	NI	NI	6320	0.332
No. 6	NI, ASL	NI, ASL	SSL	NI	5802	0.311
No. 7	NI	NI	NI	NI, ASL	6838	0.366
No. 8	NI	NI	SSL	NI, ASL	6311	0.342
No. 9	NI, ASL	NI, SSL	NI	NI, ASL	5852	0.315
No. 10	NI, ASL	NI, ASL	NI	NI, ASL	5817	0.308

NI = Numerical integration. SSL = Synchronous SL. ASL = Asynchronous SL. #LUTs = Number of look-up tables. POW = Power consumption estimated by the design suite.

The olfactory bulb model has the following membrane potentials of mitral cells and granule cells M_i , and G_i .

$$M_i, G_i, P_m, Q_g \in \mathbf{N}_N.$$

ASL dynamics of olfactory bulb model:

$$\begin{aligned} \text{If } C_m = \uparrow, \text{ then} \\ \begin{cases} M_i := F_m(M_i, M_j, G_j, P_m), \\ P_m := F_p(M_i, M_j, G_j, P_m). \end{cases} \end{aligned} \quad (9)$$

$$\begin{aligned} \text{If } C_g = \uparrow, \text{ then} \\ \begin{cases} G_i := F_g(M_j, G_i, Q_g), \\ Q_g := F_q(M_j, G_i, Q_g). \end{cases} \end{aligned} \quad (10)$$

where, j indicates the past time defined by $j = i - 1$. The functions F_m, \dots, F_q are designed in my master's thesis except for l_{ol} . For example, Fig. 5-6 shows a simulation result showing responses of the olfactory bulb model of parameter $c = 0.25$. We implemented the same procedure while changing the parameter c . The details of the results was described in the master's thesis.

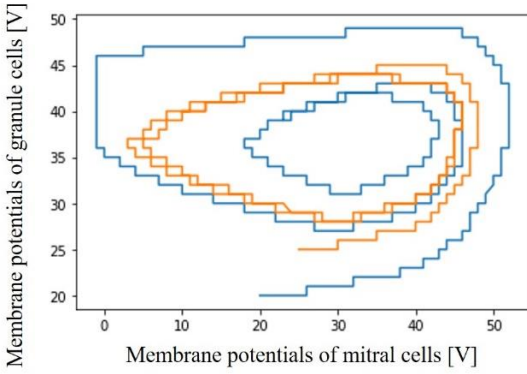


Fig. 5 : Simulation result showing responses of the mammal models to the stimulation $c = 0.25$ by asynchronous SL.

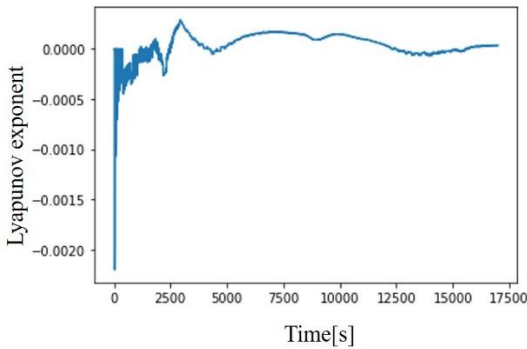


Fig. 6 : Simulation result showing the Lyapunov exponent of the mammal models to the stimulation $c = 0.25$ by asynchronous SL.

VI. Implementation and Comparisons

The dynamic equations of the presented mammal model were handwritten as python and C language

codes. The set of these codes were compiled by Jupyter Notebook and Xilinx's design suite Vitis and the resulting bitstream file was downloaded to Xilinx's field programmable gate array (FPGA) device XC7Z020-1CLG400C and XC7A100T-1CSG324C. It was confirmed that the implemented model designed the membrane potential in Section V-VII. For comparison, the olfactory bulb model of mammal was implemented as summarized in Table 2-3. The olfactory bulb model of mammal with the asynchronous SL is the presented model. In both cases, it can be confirmed that the olfactory bulb model with Asynchronous SL is the lower power than that one of numerical integration. Therefore, the asynchronous SL is more suited to implement the olfactory bulb model compared to the numerical integration.

VII. Overall Conclusions

In this paper, the novel central nervous system model of the *C. elegans* was designed by the novel design concept "design of a neuromorphic circuit based on hybrid nonlinear dynamics of asynchronous SL, synchronous SL, and numerical integration", and the novel olfactory bulb model of mammal was designed by the novel design concept "design of a neuromorphic circuit based on nonlinear dynamics of asynchronous SL." It was shown that the presented model could realize the typical decision making functions (chemotaxis) of the *C. elegans*, and the observation of chaos in the olfactory bulb. It was also shown that the presented model (no. 1) consumed the fewer circuit elements and the lower power compared to various central nervous system models of the *C. elegans* including the straightforward numerical integration model (no. 2). It was shown that the asynchronous SL model consumed the lower power compared to the olfactory bulb models of mammal including the straightforward numerical integration model. These results suggest that the results of this paper will be fundamental ingredients to design hardware-efficient brain-inspired robotics and computing. Problems for these future developments include: (a) development of a central nervous system model of a higher order organism based on the hybrid dynamics of SL and numerical integration, (b) development of a systematic analysis method of the hybrid dynamics.

Acknowledgments

I would like to express my deepest gratitude to Prof. Hiroyuki Torikai of the Dept. of Electrical Engineering, Hosei University, for his careful guidance regarding the contents and policies of this research. I would also like to thank everyone in the Torikai laboratory for their help in my daily life. Thank you very much.

Table 2 : Comparisons with PINQ

Parameter value of c	Energy[W _s] of Numerical Integration	Energy[W _s] of Asynchronous SL
-0.44	1.699	0.940
-2.52	1.532	0.729
0.25	1.437	0.481
0.32	1.428	1.006
1.42	1.441	1.154
1.91	1.616	0.519

Table 3 : Comparisons with Vitis

Parameter value of c	Energy[W _s] of Numerical Integration	Energy[W _s] of Asynchronous SL
-0.44	0.31	0.27
-2.52	0.29	0.28
0.25	0.32	0.27
0.32	0.28	0.27
1.42	0.29	0.21
1.91	0.28	0.26

Reference

- [1] <https://commons.wikimedia.org/>
- [2] J. G. White, et al., : The structure of the nervous system of the nematode *Caenorhabditis elegans*, *Phil. Trans. R. Soc. Lond. B*, vol. 314, no. 1165, pp. 314-340, 1986.
- [3] P. A. Appleby, : A model of chemotaxis and associative learning in *C. elegans*, *Biological Cybernetics*, vol. 106, no. 6-7, pp. 373-387, 2012.
- [4] T. C. Ferree and S. R. Lockery, : Computational Rules for Chemotaxis in the Nematode *C. elegans*, *Journal of Computational Neuroscience*, vol. 6, pp. 263-277, 1999.
- [5] N. A. Dunn and S. Lockery, et al., : A Neural Network Model of Chemotaxis Predicts Functions of Synaptic Connections in the Nematode *Caenorhabditis elegans*, *Journal of Computational Neuroscience*, vol. 17, pp. 137-147, 2004.
- [6] I. Mori, : Genetics of chemotaxis and thermotaxis in the nematode *caenorhabditis elegans*, *Annu. Rev. Genet.*, vol. 33, pp. 399-422, 1999.
- [7] A. V. Demin and E. E. Vityaev, : Learning in a virtual model of the *C. Elegans* nematode for locomotion and chemotaxis, *Biologically Inspired Cognitive Architectures*, vol. 7, no. 1, pp. 9-14, 2014.
- [8] P. Machado, et al., : *Si elegans*: Evaluation of an innovative optical synaptic connectivity method for *C. elegans* Phototaxis using FPGAs, *Proc. IEEE-INNS IJCNN*, pp. 185-191, 2016.
- [9] P. Machado, et al., : *Si elegans*: FPGA Hardware Emulation of *C.elegans* Nematode Nervous System, *Proc. IEEE-INNS IJCNN*, pp. 65-71, 2014.
- [10] N. Agarwal, et al., : *C. elegans* Neuromorphic Neural Network Exhibiting Undulating Locomotion, *Proc. IEEE-INNS IJCNN*, pp. 3912-3921, 2017.
- [11] S. Santurkar and B. Rajendran, : *C. elegans* chemotaxis inspired neuromorphic circuit for contour tracking and obstacle avoidance, *Proc. IEEE-INNS IJCNN*, pp. 1-8, 2015.
- [12] K. Appiah, et al., : *C. elegans* behavioral response germane to hardware modelling, *Proc. IEEE-INNS IJCNN*, pp. 4743-4750, 2016.
- [13] E. M. Izhikevich, : *Dynamical Systems in Neuroscience, The Geometry of Excitability and Bursting*, The MIT Press, July 4, 2005.
- [14] T. M. Morse, et al., : Robust Spatial Navigation in a Robot Inspired by Chemotaxis in *Caenorhabditis elegans*, *Adaptive Behavior*, vol. 6, no. 3/4, pp. 393-410, 1998.
- [15] C. D. Schuman, et al., : A Survey of Neuromorphic Computing and Neural Networks in Hardware, [arXiv:1705.06963v1](https://arxiv.org/abs/1705.06963v1).
- [16] <https://www.google.com/url?sa=i&url=https%3A%2F%2Fnatgeo.nikkeibp.co.jp%2Fimg%2Farticle%2Fnews%2F14%2F280%2F&psig=AOvVaw31QpqdWUQzyeZzYtyrbafr&ust=1674593048037000&source=images&cd=vfe&ved=0CBAQjRxqFwoTCPCBp7DH3vwCFQAAAAAdAAAAABAs>
- [17] P. Erdi, and T. Grobler, et al., : Dynamics of the olfactory bulb: bifurcations, learning, and memory, *Biological Cybernetics*, May, 1993.
- [18] Z. Li and J. J. Hopfield, : Modeling the Olfactory Bulb and its Neural Oscillatory Processings, *Biological Cybernetics*, May, 1989.
- [19] C. Alan, and L. T. Petreanu, et al., : Becoming a new neuron in the adult olfactory bulb, *Nature Publishing Group*, 2003.
- [20] E. Barnard, : Analysis of the Lynch-Granger Model for Olfactory Cortex, *Biological Cybernetics*, May, 1989.
- [21] Steven. L., : Relation of olfactory bulb and cortex. I. Spatial variation of bulbocortical interdependence, *Elsevier, Brain research*, 409, pp. 285-293, 1987.
- [22] W. J. Freeman, : Nonlinear Gain Mediating Cortical Stimulus-Response Relations, *Biological Cybernetics*, May, 1979.
- [23] Z. Li, : A Model of Olfactory Adaptation and Sensitivity Enhancement in the Olfactory Bulb, *Biological Cybernetics*, May, 1990.
- [24] K. Takeda and H. Torikai, : A novel hardware-oriented recurrent network of asynchronous CA neurons

for a neural integrator, *IEEE Trans. Circuits Syst. II*, vol. 68, no. 8, pp. 2972-2976, 2021.

[25] K. Takeda and H. Torikai, : A novel asynchronous CA neuron model: Design of neuron-like nonlinear responses based on novel bifurcation theory of asynchronous sequential logic circuit, *IEEE Trans. Circuits Syst. I*, vol. 67, no. 6, pp. 1989-2001, 2020.

[26] K. Takeda and H. Torikai, : A Novel Hardware-Efficient Central Pattern Generator Model Based on Asynchronous Cellular Automaton Dynamics for Controlling Hexapod Robot, *IEEE Access*, vol. 8, pp. 139609-139624, 2020.

[27] T. Naka and H. Torikai, : A Novel Generalized Hardware-Efficient Neuron Model based on Asynchronous CA Dynamics and its Biologically Plausible On-FPGA Learnings, *IEEE Trans. Circuits and Syst. II*, vol. 66, no. 7, pp. 1247-1251, 2019.

[28] K. Takeda and H. Torikai, : A novel hardware-efficient CPG model based on asynchronous cellular automaton, *IEICE Electron. Express*, vol. 15, no. 11, pp. 1-11, 2018.

[29] K. Takeda and H. Torikai, : A Novel Hardware-Efficient Cochlea Model Based on Asynchronous Cellular Automaton Dynamics: Theoretical Analysis and FPGA Implementation, *IEEE Trans. Circuits and Syst. II*, vol. 64, no. 9, pp. 1107-1111, 2017.

[30] T. Matsubara and H. Torikai, : An Asynchronous Recurrent Network of Cellular Automaton-based Neurons and its Reproduction of Spiking Neural Network Activities, *IEEE Trans. NNLS*, vol. 27, no. 4, pp. 836-852, 2016.

[31] N. Shimada and H. Torikai, : A Novel Asynchronous Cellular Automaton Multi-Compartment Neuron Model, *IEEE Trans. Circuits and Syst. II*, vol. 62, no. 8, pp. 776-780, 2015.

[32] T. Matsubara and H. Torikai, : Asynchronous Cellular Automaton-Based Neuron, Theoretical Analysis and On-FPGA Learning, *IEEE Trans. NEURAL NETWORKS AND LEARNING SYSTEMS*, vol. 24, no. 5, pp. 736-748, 2013.

[33] T. Noguchi and H. Torikai, : Ghost Stochastic Resonance from Asynchronous Cellular Automaton Neuron Model, *IEEE Trans. Circuits and Syst. II*, vol. 60, no. 2, pp. 111-115, 2013.